Title
Interactions between BRCA2 and RAD51 for promoting homologous recombination in Leishmania infantum.

Journal
Nucleic acids research, 40(14)

ISSN
0305-1048

Authors
Genois, Marie-Michelle
Mukherjee, Angana
Ubeda, Jean-Michel
et al.

Publication Date
2012-08-01

DOI
10.1093/nar/gks306

Peer reviewed

6570–6584 *Nucleic Acids Research, 2012, Vol. 40, No. 14* *Published online 13 April 2012*
doi:10.1093/nar/gks306

Interactions between BRCA2 and RAD51 for promoting homologous recombination in *Leishmania infantum*

Marie-Michelle Genois[1,2], Angana Mukherjee[2], Jean-Michel Ubeda[2], Rémi Buisson[1], Eric Paquet[1], Gaétan Roy[2], Marie Plourde[2], Yan Coulombe[1], Marc Ouellette[2] and Jean-Yves Masson[1,*]

[1]Genome Stability Laboratory, Laval University Cancer Research Center, Hôtel-Dieu de Québec, 9 McMahon, Québec, G1R 2J6 and [2]Centre de Recherche en Infectiologie, CHUL, 2705 Boul. Laurier, Québec, G1V 4G2, Canada

Received February 18, 2012; Revised March 21, 2012; Accepted March 22, 2012

ABSTRACT

In most organisms, the primary function of homologous recombination (HR) is to allow genome protection by the faithful repair of DNA double-strand breaks. The vital step of HR is the search for sequence homology, mediated by the RAD51 recombinase, which is stimulated further by proteins mediators such as the tumor suppressor BRCA2. The biochemical interplay between RAD51 and BRCA2 is unknown in *Leishmania* or *Trypanosoma*. Here we show that the *Leishmania infantum* BRCA2 protein possesses several critical features important for the regulation of DNA recombination at the genetic and biochemical level. A *BRCA2* null mutant, generated by gene disruption, displayed genomic instability and gene-targeting defects. Furthermore, cytological studies show that *Li*RAD51 can no longer localize to the nucleus in this mutant. The *Leishmania* RAD51 and BRCA2 interact together and the purified proteins bind single-strand DNA. Remarkably, *Li*BRCA2 is a recombination mediator that stimulates the invasion of a resected DNA double-strand break in an undamaged template by *Li*RAD51 to form a D-loop structure. Collectively, our data show that *Li*BRCA2 and *Li*RAD51 promote HR at the genetic and biochemical level in *L. infantum*, the causative agent of visceral leishmaniasis.

INTRODUCTION

DNA double-strand breaks (DSBs) are one of the most cytotoxic lesions that can occur in the genomic DNA. In human cells, these lesions are repaired by non-homologous end joining (NHEJ) but also homologous recombination (HR). In this context, HR protects the genome from DNA translocations or rearrangements. Several studies have demonstrated a role for RAD51 and BRCA2 in both mitotic and meiotic recombination. BRCA2 plays a pivotal role in controlling the function and localization of RAD51 during HR, a central process for the maintenance of genome stability and cancer prevention (1). The BRC repeats located at the center of BRCA2 confer a very sophisticated mode of regulation. Indeed, the BRC repeats bind RAD51 and control RAD51 nucleoprotein filament formation in conjunction with the BRCA2 DNA-binding domain, whereas a BRC-unrelated RAD51-binding motif located at the C-terminus of BRCA2 appears to stabilize the filament (2–5). BRCA2 contains also a characteristic OB (oligonucleotide/oligosaccharide-binding) pocket, which consists of a highly curved five-stranded β-sheet that closes on itself to form a β-barrel, which confers single-strand DNA (ssDNA)-binding activity (6,7). Orthologs of BRCA2 have been found in eukaryotes such as human, mouse, rat, Xenopus, *Caenorhabditis elegans*, *Trypanosoma* and *Leishmania* but this protein is absent from yeast, archaea and bacteria (8). *Saccharomyces cerevisiae* does not bear a BRCA2 homolog, a function that might be replaced by RAD52. However, RAD52 orthologs have not been detected in *Leishmania infantum*, although these enzymes have a central role in recombination and DNA repair (9). Budding yeast or human RAD52 promote single-strand annealing of complementary ssDNA independent of RAD51 (10,11) and enhance RAD51-mediated strand invasion by direct interaction with the recombinase RAD51 (12). Although the NHEJ factors Ku70 and Ku80 have been identified in trypanosomes (13,14), it is not clear whether these human parasites possess a NHEJ activity as no DNA ligase IV and XRCC4 homologs were detected within their genomes (15).

*To whom correspondence should be addressed. Tel: +1 418 525 4444 (15154); Fax: +1 418 691 5439; Email: Jean-Yves.Masson@crhdq.ulaval.ca

The most common view in the control of the HR process is that HR should be suppressed up to a level where genomic stability is maintained. However, organisms such as *Trypanosoma brucei* use HR as a beneficial mechanism for antigenic variation (16) or *Leishmania* for drug resistance (17). First, it has been assumed that HR and DSB formation play an important role in antigenic variation. Variant surface glycoprotein (VSG) switching allows some of the infecting *T. brucei* to evade the host immune response, therefore allowing survival of the parasite and new transmission to another mammal. Analysis in *T. brucei* revealed that VSG switching frequency is highly dependent on RAD51 and BRCA2 proteins. Moreover, it was shown that the induction of a DSB adjacent to the 70-bp repeats upstream of the transcribed VSG induced VSG switching. The switching frequency was increased 250-fold compared to control cells without an I-SceI recognition sequence. Interestingly, VSG switching occurred through break-induced replication (16). Hence, understanding the biochemical role of BRCA2 in HR might be beneficial in understanding trypanosomatid diseases. Moreover, *L. infantum* amplify regions of its genome upon drug selection by HR between homologous repeated sequences (17).

The large size of the human BRCA2 protein (384 kDa) poses a great technical challenge for biochemical analyses. Amongst all BRCA2 proteins, Brh2 of *Ustilago maydis*, has been extensively characterized because of its smaller size (127 kDa). Brh2 binds D-loops specifically (18) and promotes strand invasion in an homologous duplex (19). Brh2 facilitates the second-end capture step in the DNA DSB model, by enhancing the annealing of a second complementary single-strand to the displaced strand of a D-loop to form a duplexed D-loop (20). It was recently reported that the human BRCA2 protein forms rings on DNA (21), binds to approximately six RAD51 molecules and promotes RAD51 filament formation on RPA-covered ssDNAs (22). In addition, it stimulates RAD51-mediated DNA strand exchange (23). To date, however, D-loop formation was not performed for the human BRCA2 protein (21–23) and evidence of human BRCA2 being able to stimulate RAD51-mediated D-loop formation is lacking.

The *Rad51* gene from the parasite *Leishmania major* has been identified previously (24). Comparative bioinformatic analyses revealed that the size of the *L. infantum* BRCA2 protein was about three times smaller (125 kDa) than its human counterpart. Moreover, our analyses revealed that *Li*BRCA2 possesses key features of the BRCA2 family. We exploited the smaller size of the *Leishmania* BRCA2 protein to better understand its function in HR, along with the *Li*RAD51 recombinase.

MATERIALS AND METHODS

Nucleic acids

The *L. infantum Brca2* and *Rad51* genes were amplified by PCR from genomic DNA as protein-encoding genes are intronless in *Leishmania*. The sequences were identical to the NCBI reference sequences A4HYJ9 and A4I3C9, respectively. The *LiBrca2* PCR fragment was obtained with the combination of primers JYM1599 and JYM1600 (Supplementary Table S1) and the purified PCR fragment was cloned in a modified pFASTBAC1 plasmid (Invitrogen) encoding GST and His tags to yield the GST–*Li*BRCA2–HIS construct. Similarly, *LiRad51* was amplified with primers JYM1669 and JYM1670 (Supplementary Table S1) then cloned in a modified pFASTBAC1 plasmid (Invitrogen) encoding GST to generate the *Li*RAD51–GST construct. *Li*BRCA2–GFP was obtained following the amplification of *LiBrca2* with primers JYM1894 and JYM1896 (Supplementary Table S1) and the resulting PCR product was cloned in the *Leishmania* expression vector pSPαHYGαGFP. Finally, the *Li*RAD51–DsRed version was generated with primers JYM1899 and JYM1900 (Supplementary Table S1), and the purified PCR product was cloned in the pSP72αNEOα-DsRed vector (constructed by inserting DsRed in pSP72αNEOα (25)).

Generation of the *LiBrca2* null mutant

To generate a single knockout of *LiBrca2* (e.g. *LinJ.20.0070* in geneDB see http://www.genedb.org/), the entire ORF of *LinJ.20.0070* was substituted by a neomycin phosphotransferase cassette flanked by 5′- and 3′-regions of *LinJ.20.0070*. The upstream *LiBrca2* region was amplified with primers MOU1001 and MOU1002 (Supplementary Table S1), and the *LiBrca2* downstream region was obtained with primers combination MOU1003 and MOU1004 (Supplementary Table S1). Targeting flanks were amplified from *L. infantum* genomic DNA and ligated to the *NEO* marker gene as previously reported (26). An insertional inactivation strategy was performed to target the second *LiBrca2* allele. A polypyrimidine stretch (Y)-hygromycin-a-tubulin fragment (Y*HYG*a) was obtained by PCR with the primers MOU1005 and MOU1006 of the *Leishmania* expression vector psp72Yhygroa (27). The Y*HYGa* purified fragment was then fused with the 5′- and 3′-flanking regions of *LiBrca2* after their respective PCR amplification with primers MOU1007 and MOU1008 (upstream region) and MOU1009 and MOU1010 (downstream region) (Supplementary Table S1). The final targeting cassette was inserted into the ORF of *LinJ.20.0070* by HR. For episomal complementation of *LinJ.20.0070*, the *LiBrca2* gene was amplified using 1 ng of *L. infantum* genomic DNA, with two primers containing either *XbaI* (MOU 1011) or *SalI* (MOU1012) (Supplementary Table S1) restriction sites. The PCR product was first cloned in the pGEM-T Easy vector then the construct was digested with both restriction enzymes. The *LiBrca2* fragment was subcloned into the *Leishmania* expression vector pSP72α*ZEO*α (28) within the *XbaI* and *SalI* cloning sites. All constructs were confirmed by DNA sequencing. The empty vector pSP72α*ZEO*α was transfected in *L. infantum* wild-type cells (LiWT) and in the *LinJ.20.0070* null mutant (*LinJ.20.0070*$^{-/-}$) and these cells were used as controls.

Recombinants and transfectants were selected as following: 5 μg of both linear inactivation cassettes (neo or

hyg) were obtained by PCR amplification, purified and transfected into promastigotes by electroporation as previously reported (25). For plasmid transfection (episomal complementation or empty vector), 10–20 μg was used. Recombinants and transfectants were selected in the presence of 300 μg/ml hygromycin B, 40 μg/ml G418 (Geneticin, Gibco-BRL) and 800 μg/ml zeocin (Invitrogen) depending on the marker used. After 2–3 passages, cells resistant to the antibiotic selection were cloned on SDM–agar plates (1%) in the presence of 20 μg/ml of G418 or 160 μg/ml of hygromycin B. Clones were picked up after 7–10 days and used for analysis. PCR analysis of three different clones after integration of the *HYG* and *NEO* cassettes was done using primers pairs a + b, c + d, e + f respectively MOU1007 + MOU1110, MOU1113 + MOU1114, MOU1115 + MOU1116 (Supplementary Table S1).

Southern blot analysis

Genomic DNA of the selected clones was isolated using DNAzol as recommended by the manufacturer (Invitrogen). Digested genomic DNAs with *ApaI* and *ClaI* were subjected to Southern blot hybridization with [α-^{32}P]dCTP-labeled DNA probes according to standard protocols (29). All probes were obtained by PCR from *Leishmania* genomic DNA or from plasmids containing markers then purified appropriately before being labeled.

Transformation efficiency

We used the construct 5′-GSH1-BLA-3′GSH1 (26) to target the single copy gene *GSH1* on chromosome 18 and confer blasticidin resistance in order to monitor the integration efficiency. Briefly, 4×10^7 cells of WT pSP72α*ZEO*α, *LinJ.20.0070*$^{-/-}$ pSP72α*ZEO*α, and *LinJ.20.0070*$^{-/-}$ pSP72α*ZEO*α encoding *Li*BRCA2 were transfected with 5 μg of the linear 5′GSH1-BLA-3′GSH1 construct and after 24 h following electroporation, cells were preselected with 40 μg/ml blasticidin. After another 24 h cells were plated on SDM–agar plates (1% agar and 100 μg/ml blasticidin). *Li*WT cells and complemented cells were plated at a density of 5×10^6 cells/plate and the null mutant *LinJ.20.0070* $^{-/-}$ at 7×10^6 cells. All these strains were also transfected with an empty plasmid (pSPαBLAαGSH1) as a control. Colonies were counted after 10–15 days of plating. Genomic DNA was extracted from selected clones using the DNAzol method (Invitrogen) and integration of the *BLAST* marker gene (*BLA*) into the *GSH1* chromosomal locus was confirmed by PCR (primers MOU1117 and MOU1118) (Supplementary Table S1).

Western blotting of *Li*RAD51 and *Li*BRCA2 in *Leishmania* protein extracts

Leishmania infantum promastigotes were grown in SDM–79 medium supplemented with 10% heat-inactivated fetal bovine serum, 5 μg/ml hemin and 5 μM biopterin at pH 7.0, 28°C up to the logarithmic phase ($OD_{600\,nm} \sim 0.5$). Cultures containing 5×10^6 cells resuspended in 5 ml medium were prepared with 12 μg/ml of phleomycin and incubated at 28°C for 0, 24, 48, 72 and 96 h. At each time point, the cells were centrifuged at 3000 rpm for 5 min, washed once with HEPES/NaCl buffer (21 mM HEPES, pH 7.2, 137 mM NaCl, 5 mM KCl, 0.7 mM Na_2HPO_4, 6 mM glucose) then resuspended in 30 μl of 2× Laemmli buffer. The protein samples (20 μl) were loaded onto a 8% SDS–PAGE and analyzed by western blot using the indicated antibodies. *Li*BRCA2 and hRAD51 antibodies were generated in the laboratory and were used at 1:5000 concentration whereas the α-tubulin antibody was purchased from Abcam and used at 1: 2500 dilution.

Protein sequence analysis

The domains presented in the Supplementary Figure S1 were identified using pfam with an *E*-value cutoff of 10 (30). The phylogenetic tree was generated by first gathering BRC repeat sequences for each different species. The sequences corresponding to the BRC repeat domain in each protein was extracted and numbered in function of their location relative to the N-terminal of the protein so the closest domain in N-terminal is assigned number 1. The alignment used in Supplementary Figure S1B is the alignment reported by hmmsearch when aligning sequence to the model. The phylogenetic tree of Supplementary Figure S1B was generated within Jalview using Neighbor-joining with the Blosum 62 scoring matrix (31). The tree reported in Supplementary Figure S1C was generated on a selected portion of global multiple alignment produced using the software MAFFT in FFT-NS-i mode (32,33). We selected the portion located just before OB1 (human starting amino acid S2590). The tree building option on the MAFFT website was used to produce the tree of Supplementary Figure S1C using the Neighbor-joining method with JTT substitution model without heterogeneity among sites and 1000 bootstraps.

Fluorescence microscopy

Promastigote cells expressing the green fluorescence protein (GFP)-fusion proteins or DsRed-fusion proteins were first washed with HEPES/NaCl buffer then incubated 10 min with 0.5 μg/ml DAPI (Sigma) in the dark. The cells were washed twice with HEPES/NaCl buffer and immobilized in HEPES/NaCl buffer containing 10% glycerol. Live parasites were mounted on microscope slides with coverslips sealed with nail varnish and air-dried for 15 min. The slides were visualized by epifluorescence microscopy. Bright field and fluorescence images were taken using a Nikon Eclipse TE300 inverted microscope equipped with a Photometrics coolSNAPfx camera. Visualization of the DAPI, GFP and DsRed fluorophores were achieved using respectively 340/380 nm, 460/500 nm, 532/588 nm excitation filters and 435/485 nm, 510/560 nm, 607/683 nm emission filters with a 100× objective. The images were processed using ImageJ version 1.42 (National Institutes of Health, USA; http://rsb.info.nih.gov/ij).

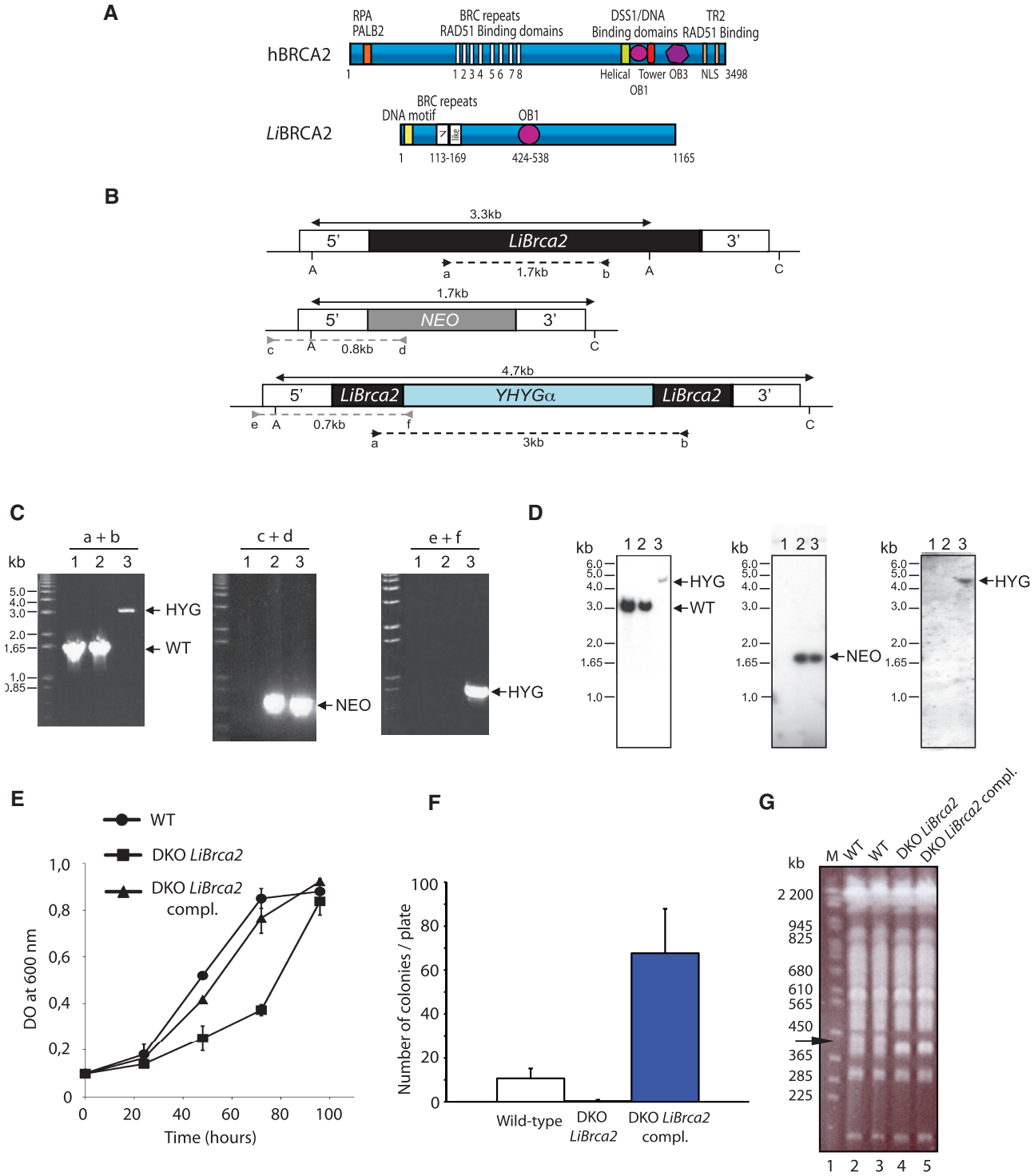

Figure 1. Inactivation of *LiBrca2* and phenotypic analyses. (**A**) Schematic representation of *Li*BRCA2 in comparison to human BRCA2. BRC repeats, OB-folds, and RAD51-binding regions are shown. (**B**) Schematic representation of the *LiBrca2* chromosomal locus (top) and inactivation cassettes with the neomycin phosphotransferase (*Neo,* middle) and hygromycin phosphotransferase (*Hyg*, bottom) markers. The position of the primers pairs (a + b, c + d, e + f) used in (**C**) is depicted. (C) PCR analysis of three different clones after integration of the *HYG* and *NEO* cassettes. Clone in lane 1 is identical to *L. infantum* WT (e.g. no integration), clone in lane 2 has a *NEO* insertion in one allele, and clone in lane 3 has both *NEO*/*HYG* insertions. (**D**) Southern blots of three different clones digested with *ApaI* (A) and *Cla*I (C) after hybridizing with a 700 bp specific *LiBrca2* (left), *NEO* (middle) and *HYG* probes (right) on the DNA isolated from the three clones described in (C). (**E**) Growth retardation of *LiBrca2* null mutants grown as promastigotes. Growth of *L. infantum* WT (closed circles), DKO *LiBrca2* (closed squares), and DKO *LiBrca2* complemented with a plasmid expressing *Li*BRCA2 (closed triangles), was measured over time. (**F**) Inactivation of *LiBrca2* impairs gene targeting. Gene targeting was measured in *L. infantum* WT, DKO *LiBrca2* and DKO *LiBrca2* complemented with a plasmid expressing *Li*BRCA2. (**G**) DKO *LiBrca2* cells display genomic instability. Pulsed field gel electrophoresis was performed on *L. infantum* WT cells (lanes 2 and 3), DKO *LiBrca2* (lane 4) and DKO *LiBrca2* complemented with a plasmid expressing *Li*BRCA2 (lane 5). The arrow shows a chromosomal band present in WT cells but absent in the other strains. Molecular weight markers (BioRad, *S. cerevisiae* DNA size standard) were used in lane 1.

Purification of human RPA, human RAD51 and *L. infantum* RAD51 and BRCA2

The human RPA protein was purified according to (34), and human RAD51 was purified as described in (35). GST–*Li*BRCA2–His was purified from baculovirus-infected Sf9 cells. Sf9 insect cells (1 l culture) were infected with the BRCA2 baculovirus for 3 days at 27°C. The cell pellet (600 ml) was resuspended in 18 ml of PBS washing buffer [300 mM NaCl, 1 mM EDTA, 0.05% Triton, 1 mM DTT in 1× PBS (GIBCO)] containing protease inhibitors PMSF (1 mM), aprotinin (0.019 UIT/ml) and leupeptin (1 μg/ml). The suspension was lysed using a Dounce homogenizer (15 strokes), sonicated three times for 30 s on ice. Insoluble material was removed by centrifugation in small aliquots of 1 ml (10 min, 13 000 rpm, 4°C). An amount of 1 ml of glutathione sepharose beads (GE Healthcare) was added to the combined supernatant and incubated during 1 h at 4°C. The beads were washed two times with 1× PBS then incubated for 30 min in HSP buffer (5 mM ATP, 15 mM $MgCl_2$ in 1× PBS) at 4°C. The beads were further washed two times with 1× PBS containing 500 mM NaCl and one more time in the Talon buffer (50 mM $NaHPO_4$ pH 7.0, 500 mM NaCl, 10% glycerol, 0.05% Triton, 5 mM imidazole). The *Li*BRCA2 protein was eluted by cleavage with PreScission protease (60 U/ml, GE Healthcare) during 3 h at 4°C in the Talon buffer. The supernatant was added on 200 μl of Talon resin (Clontech) and incubated for 30 min at 4°C. The resin was washed two times with 4 ml of Talon buffer containing 30 mM imidazole and one time with 80 mM imidazole. *Li*BRCA2 protein was eluted in buffer containing 500 mM imidazole and dialyzed in storage buffer (20 mM Tris–Acetate, pH 8.0, 200 mM KOAc, 10% glycerol, 1 mM EDTA, 0.5 mM DTT). The GST–*Li*RAD51 protein was purified as for GST–*Li*BRCA2–His but excluding the Talon purification step. The beads were washed in PreScission washing buffer (50 mM Tris–HCl pH 7.4, 150 mM NaCl, 1 mM EDTA, 1 mM DTT, 0.05% Tween 20) before cleavage. The *Li*RAD51 protein was eluted following an overnight cleavage at 4°C with 60 U/ml of PreScission protease (GE Healthcare) in PreScission washing buffer.

Gel-filtration analysis

The molecular mass of *Li*RAD51 (20 μg) and *Li*BRCA2 (5 μg) were determined by gel filtration using 250 μg of a series of protein standards; bovine thyroglobulin (670 kDa), bovine gamma globulin (158 kDa), chicken ovalbumin (44 kDa), horse myoglobin (17 kDa) and vitamin B-12 (1.35 kDa). Purified proteins were analyzed on a FPLC Explorer 10 system fitted with a 24 ml Superdex 200 PC 3.2/30 column (Pharmacia) equilibrated in gel-filtration buffer (25 mM Tris–HCl pH 7.5, 150 mM KCl, 5% glycerol, 1 mM DTT). Fractions (500 μl) were collected and analyzed by SDS–PAGE followed by western blotting with a monoclonal anti-Histidine antibody (BD Biosciences) for *Li*BRCA2 or a polyclonal anti-human RAD51 to detect *Li*RAD51.

D-loop assays

The D-loop assay with 3′-tail DNA was conducted essentially as described (36). A linear duplex DNA was prepared by restriction digestion of pPB4.3 DNA (4.3 kb) (37) with *SmaI*. Linear DNA with 3′-tails (~200 nt in length) were generated by treatment of linearized pPB4.3 DNA (100 μg) with T7 gene 6 exonuclease (830 units, 1 min at 25°C) in 800 μl reaction volume containing 20 mM Tris–Acetate pH 7.9, 50 mM KOAc pH 7.9, 10 mM $Mg(OAc)_2$ and 1 mM DTT. Exonuclease digestion was stopped by extraction with phenol/chloroform. Finally, the resected DNA was purified by gel electrophoresis through a 0.8% (w/v) agarose gel and recovered by electroelution. ^{32}P-labeled 3′-tailed DNA substrate (1 μM nucleotides) was incubated for 5 min at 37°C with the indicated concentration of *Li*RAD51 and/or *Li*BRCA2 in 25 mM Tris–Acetate pH 7.5, 1 mM DTT, 20 mM creatine phosphate, 5 U/ml phosphocreatine kinase, 1 mM ATP and 0.5 mM $MgCl_2$ in 10 μl. CsCl-purified pPB4.3 replicative form I DNA (300 μM) was added and the reaction was incubated for 1 h 30 min. The reaction was quenched with the addition of one-fifth volume of stop buffer (20 mM Tris–Cl pH 7.5 and 2 mg/ml proteinase K) followed by a 30 min incubation period at 37°C. Labeled DNA products were analyzed by electrophoresis through a 0.8% TAE 1× agarose gel, run at 65 V, dried onto DE81 filter paper and visualized by autoradiography.

DNA-binding assays

Reactions (10 μl) contained 100 nM of ^{32}P-labeled DNA oligonucleotides (e.g. primer JYM925 for the ssDNA assay and primers JYM925/JYM945 for the double-strand DNA (dsDNA) assay, see Supplementary Table S1 for oligonucleotide sequences) and *Li*BRCA2 and/or *Li*RAD51, at the indicated concentrations, in binding buffer (20 mM Triethanolamine–HCl pH 7.5, 50 mM NaCl, 2 mM $MgCl_2$, 2 mM ATP and 1 mM DTT). Proteins were added to reactions and incubated at 37°C for 10 min, followed by 15 min of fixation with 0.2% glutaraldehyde. Reactions were loaded onto a 0.8% TBE 1× agarose gel.

Single-strand annealing reactions

Reactions (10 μl) contained denatured ^{32}P-labeled dsDNA (50 nM) with *Li*RAD51 or/and *Li*BRCA2, at the indicated concentrations, in HEPES buffer (20 mM HEPES pH 7.5, 5 mM $Mg(CH_3COO)_2$, 2 mM ATP, 5 mM DTT and 100 mM NaCl). Incubation was performed at 20°C for 10 min. The reaction products were deproteinized by the addition of one-fifth volume of stop buffer (20 mM Tris–Cl pH 7.5 and 2 mg/ml proteinase K) followed by a 10 min incubation period at 20°C. Labeled DNA products were analyzed by electrophoresis (8% PAGE gel with TBE1X buffer, run at 150 V for 3 h), the gel was dried onto DE81 filter paper and visualized by autoradiography.

Immunoprecipitation

Immunoprecipitation from purified proteins were performed as follows. Purified *Li*BRCA2 (750 ng) and hRPA (1 μg) were incubated in 100 μl of IPR buffer (20 mM Tris–acetate pH 8.0, 125 mM KOAc, 0.5 mM EDTA, 0.5% NP40, 10% glycerol, 0.1 mg/ml BSA) for 30 min at 37°C. An amount of 1 μg anti-Histidine (Clontech) was added for 30 min at 4°C followed by the addition of 15 μl protein A/G sepharose beads (Pierce) for 30 min. Immunoprecipitates were washed four times in IPR buffer containing 300 mM KOAc and visualized by western blotting using the indicated antibodies.

Sf9 insect cells (20 ml) were coinfected with the *Li*BRCA2 and *Li*RAD51 baculoviruses (dilution 1/150) for 2 days at 27°C. The cell pellet was resuspended in 5 ml of IP100 buffer (20 mM Tris–Acetate pH 8.0, 100 mM KOAc, 0.5 mM EDTA, 0.5% NP40, 10% glycerol, 0.1 mg/ml BSA, 1 mM DTT) containing protease inhibitors PMSF (1 mM), aprotinin (0.019 UIT/ml) and leupeptin (1 μg/ml). The suspension was sonicated two times for 10 s. Insoluble material was removed by centrifugation in small aliquots of 1 ml (10 min, 13 000 rpm, 4°C). 2 μg anti-Histidine (Clontech) was added to 1 mg of protein and incubated during 2 h at 4°C followed by the addition of 15 μl protein A/G sepharose beads (Pierce) for 1 h at 4°C. Immunoprecipitates were washed four times in the IP100 buffer with the indicated concentration of KOAc and visualized by western blotting using the indicated antibodies.

Biotin pull-down assay

Magnetic beads (Roche) containing 5′-biotinylated ssDNA polydT 83-mer (corresponding to the final concentration of 1 μM nucleotide) were pre-incubated with a blocking buffer (25 mM Tris–acetate pH 7.5, 40 mM KOAc, 1 mM DTT, 0.02% Igepal and 10 mg/ml BSA) for 20 min at 37°C. The beads were captured with the magnetic particle separator, washed once with DC buffer (25 mM Tris–Acetate pH 7.5, 40 mM KOAc, 1 mM DTT, 0.02% Igepal, 1 mg/ml BSA, 5 mM ATP and 0.5 mM $MgCl_2$) and resuspended in the same buffer. hRPA was added (17 μl) and the reaction was incubated for 5 min at 37°C. Then *Li*RAD51 (200 nM) was added and the reaction was incubated for 5 min at 37°C. Finally, the indicating concentration of *Li*BRCA2 protein was added (in 20 μl) and the reaction was incubated further for 5 min at 37°C. The beads were captured and were washed twice with 50 μl of washing buffer (25 mM Tris–Acetate pH 7.5, 40 mM KOAc, 1 mM DTT, 0.02% Igepal, 5 mM ATP and 0.5 mM $MgCl_2$). Finally, 15 μl of 2× Laemmli buffer was added and beads were heated 5 min at 95°C. The beads were captured again and the supernatants were loaded onto a 8% SDS–PAGE Ruby (Invitrogen) and visualized by UV.

RESULTS

Bioinformatic analyses of *Li*BRCA2

Analysis of the *Leishmania* genome suggested that *LinJ20.0070* is a BRCA2 ortholog. We scrutinized whether *Li*BRCA2 possessed features reminiscent of the BRCA2 family of enzymes. We started by first detecting all the significant protein domains within the selected list of BRCA2 proteins using pfam (30) with a permissive *E*-value. We detected two BRC repeats, one OB-fold and also at least one putative zf–RanBP (Zn-finger in Ran-binding protein) domain for every *Leishmania* species analyzed (Supplementary Figure S1B). We also detected 15, 2, 7, 8 and 4 BRC repeats for *T. brucei*, *Trypanosoma cruzi*, mouse, human and Arabidopsis, respectively. The OB-fold domain could be detected in all proteins analyzed. The helical domain could only be detected in mouse, human and Arabidopsis and the Tower domain is only present in mouse and human.

Since the BRC repeats are present in all the BRCA2 proteins, we were interested to study the evolutionary link between the BRC repeats of all the different species. For this purpose we extracted the BRC repeats detected by pfam and aligned them to produce a phylogenetic tree (Supplementary Figure S1A). All the first BRC repeats of *Leishmania* are clustering together with all the BRC repeats of *T. brucei* or *cruzi*. The second BRC repeats of *Leishmania* are forming a cluster with the two first BRC repeats of Arabidopsis. The two BRC repeats of *Leishmania* are within a cluster also composed of mouse and human BRC 3, 4, 7 and 8. We hypothesized that the two BRC repeats of all *Leishmania* species analyzed (Supplementary Figure S1A and S1B) are related to the mouse and human BRC repeats 3, 4, 7 and 8. Furthermore, we analyzed globally the evolution of the BRCA2 proteins with a phylogenetic tree produced from an alignment of all the BRCA2 proteins. We can observe from Supplementary Figure S1C that the *L. major* and *L. donovani* are the most similar form of BRCA2 followed by *L. infantum* and *L. braziliensis*. Collectively, these bioinformatic analyses strongly suggested that *L. infantum* possesses a BRCA2 homolog at amino acid and phylogenic levels. A schematic representation of *Li*BRCA2 in comparison to human BRCA2 is depicted in Figure 1A.

Inactivation of *LinJ.20.0070*, the *Leishmania* BRCA2 gene

Having established that *L. infantum* contains an homolog of BRCA2, we generated a *LiBrca2* null mutant. The BRCA2 ortholog *LinJ.20.0070* is a single copy gene. In an attempt to inactivate *LinJ.20.0070*, one gene inactivation cassette with neomycin phosphotransferase (NEO) and one gene disruption cassette with hygromycin phosphotransferase (HYG) marker (Figure 1B) were prepared. Linear NEO or HYG fragments were transfected into *L. infantum* and recombination events of clones selected on agar plates were followed by PCR reactions and Southern blot hybridizations (Figure 1C and D). Digestion with *ApaI* and *ClaI* should yield a 3.3-kb band in WT, while replacing one allele with NEO should yield a 1.7-kb fragment hybridizing to a 3′-UTR probe. Insertional inactivation with YHYGα into the second *LinJ.20.0070* allele of *LinJ.20.0070/NEO* cells and hybridizing with the same probe should yield a single

4.7-kb band. Five clones from each independent transfection were selected. The DNA of one such representative *LinJ.20.0070*/NEO (*LinJ.20.0070*$^{+/-}$) and NEO/HYG (*LinJ.20.0070*$^{-/-}$) clone was isolated, analyzed by PCR using primers (a–f) (Figure 1B). The use of primers a and b should lead to a fragment of 1.7-kb in the WT and the single knockout *LinJ.20.0070* should lead to a 3-kb fragment upon insertion of HYG (Figure 1B and C). The integration of *NEO* and *HYG* at their homologous locus were confirmed by primer pairs c + d and e + f, respectively. The DNA of these representative *LinJ.20.0070*/NEO and *NEO*/*HYG* clones were digested with *ApaI* and *ClaI* and analyzed by Southern blots after hybridizing with a 3′-UTR *LinJ.20.0070* probe, NEO and HYG probes. Bands of the expected size hybridizing with all the probes were observed (Figure 1D, lanes 1–3), confirming the generation of a BRCA2 *L. infantum* null mutant, termed DKO *LiBrca2*.

Phenotypes of *LiBrca2* null mutants

Although deletion of BRCA2 in mouse leads to an embryonic lethality phenotype (38), the *LiBrca2* mutants were viable. *LiBrca2* null mutants, adapted to *in vitro* culture, had a specific growth retardation even when grown as promastigotes in SDM medium when compared to wild-type cells (WT) (Figure 1E). This growth retardation was rescued upon the re-introduction of an episomal construct encoding BRCA2 (DKO *LiBrca*2 complemented). We have succeeded in generating an independent *BRCA2* null mutant and observed the same growth defect (data not shown).

Since gene disruption in *Leishmania* is mediated by double crossed-over HR, we sought to determine whether the loss of BRCA2 would decrease the efficiency of HR. This was assayed by measuring the transformation efficiencies of promastigotes transfected with the linear construct 5′-GSH1-BLA-GSH1-3′ (26) which integrates a blasticidin deaminase cassette into the *GSH1* locus on chromosome 18. There was at least a 10-fold decrease in the transformation frequency, as determined by colony numbering, when compared to WT (Figure 1F). Adding back an episomal BRCA2 increased the number of colonies at least to the wild-type levels and in one set of experiments to 6-fold increase in colony numbers. The number of episomal copies per cell can be variable, which might explain the differences between each experiment. The correct integration of the GSH1/BLAS cassette was tested by PCR in selected colonies (data not shown).

BRCA2 inactivation in mammalian cells causes accumulation of aberrant chromosomes, including gross chromosomal rearrangements occurring from chromosomal loss, breakage or translocations (39). The karyotype of the *L. infantum* BRCA2 null mutant was analyzed by pulsed field gel electrophoresis. Size variations were observed in chromosomes between 365 and 450 kb in DKO *LiBrca2* (Figure 1G, lane 4) compared to WT cells (Figure 1G, lanes 2 and 3). Reintroduction of BRCA2 in the null mutant did not restore chromosome integrity (Figure 1G, lane 5).

*Li*RAD51 expression is modulated by DNA damage

To date, it is unclear to what extent HR proteins are expressed in *L. infantum*. The expression of *Li*BRCA2 and *Li*RAD51 was monitored over time using western blotting in mock- or phleomycin-treated cells (Figure 2A). To do this, we used antibodies raised against *Li*BRCA2 and human RAD51 that recognized *Li*BRCA2 and *Li*RAD51, respectively. *Li*RAD51 and hRAD51 are 74.5% similar and 63% identical at the amino acid level (Supplementary Figure S2). The proteins recognized by the antibodies were at the predicted molecular weight, 41 kDa for *Li*RAD51 and 125 kDa for *Li*BRCA2. The levels of *Li*BRCA2 did not fluctuate over time in cells treated with the DNA damaging agent phleomycin. However, the levels of *Li*RAD51 were vastly induced 96 h after DNA damage. This observation is in accordance to the induction of *Lm*RAD51 expression in *L. major* promastigotes after phleomycin treatment (24).

In vivo localization of *Li*BRCA2

In human cells, RAD51 and BRCA2 are known to accumulate as foci at DNA damage sites. The formation of RAD51 foci is impaired in BRCA2-deficient cells. Furthermore, cell fractionation assays using CAPAN-1 cells (which contains BRCA2 6174delT, a truncated version), revealed that RAD51 is present in majority in the cytoplasm, rather than the nuclear fraction (2). We therefore investigated whether these functions are conserved in *Leishmania* species. To do this, we expressed *Li*RAD51 fused to DsRed and *Li*BRCA2 fused to GFP. When both *Li*BRCA2–GFP and *Li*RAD51–DsRed were expressed in WT *Leishmania* cells, both *Li*RAD51 and *Li*BRCA2 colocalized in the nucleus (Figure 2B and Supplementary Figure S3A). The expression of GFP or DsRed alone in *L. infantum* lead to a much different pattern of staining than *LiBRCA2*–GFP and *LiRAD51*–DsRed (Supplementary Figure S3B). Interestingly, *Li*RAD51 was no longer found in the nucleus in the absence of *Li*BRCA2, but in the cytosol as part of several punctuated stained regions (Figure 2C and Supplementary Figure S3C). These results show that *Li*BRCA2, like human BRCA2, control the nuclear accumulation of *Li*RAD51.

Expression and purification of *L. infantum* RAD51 and BRCA2

To open the door to biochemical studies of *L. infantum* RAD51 and BRCA2, we purified these proteins to homogeneity. First, the *Li*RAD51 and *Li*BRCA2 genes were amplified by PCR from *L. infantum* genomic DNA and cloned in pET16b vector. Following expression of *Li*BRCA2 in *Escherichia coli*, very low expression was achieved, and *Li*BRCA2 was highly degraded after Talon purification (data not shown). Therefore, we developed a two-step affinity purification procedure to purify full length *Li*BRCA2 without any degradation products. *LiBrca2* gene was cloned in a modified pFASTBAC vector to add, respectively, a glutathione-S-transferase tag at the N-terminus and a 10-histidine

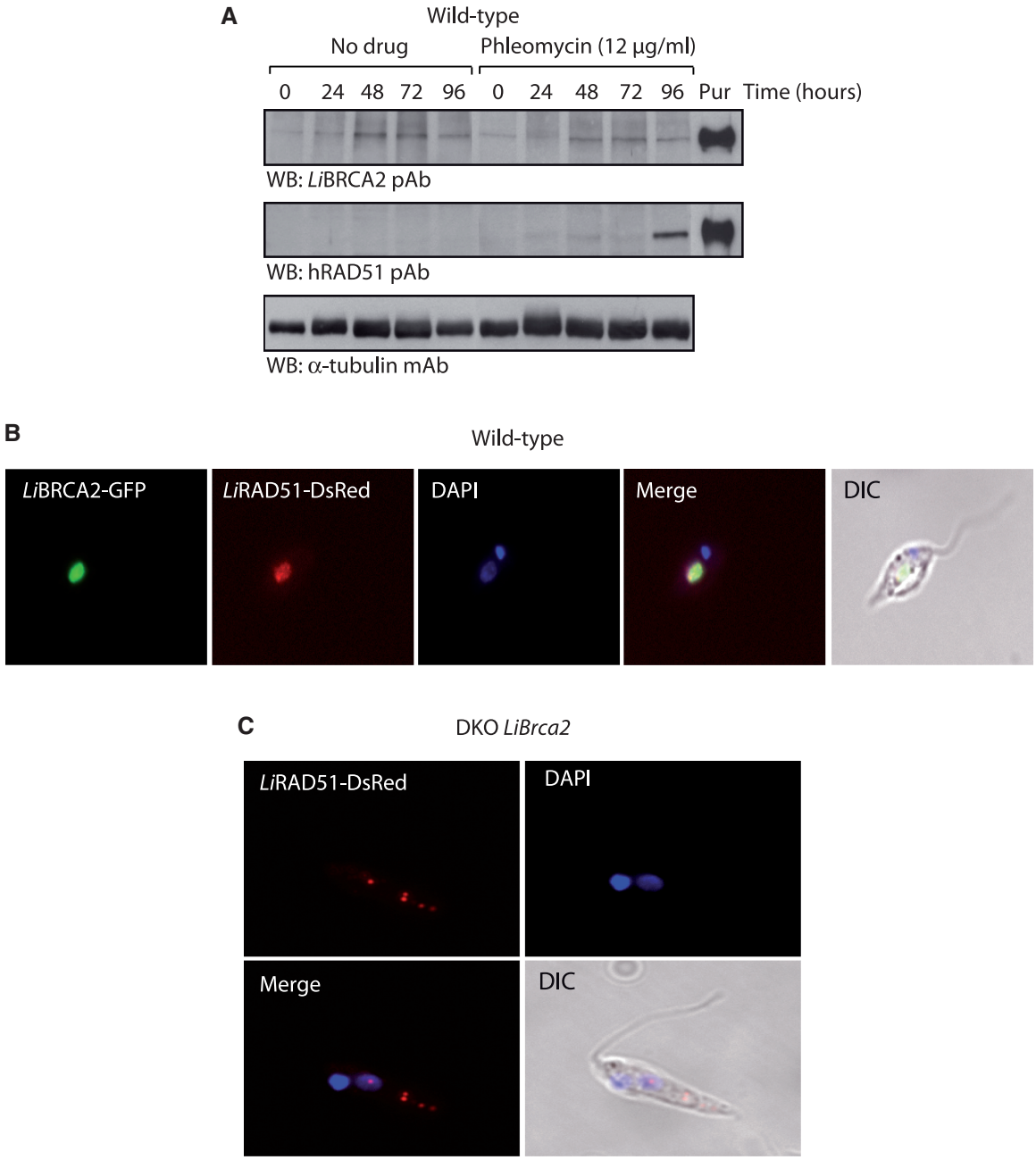

Figure 2. Expression and cytological analysis of *Li*RAD51 and *Li*BRCA2. (**A**) Phleomycin treatment induces *Li*RAD51 expression in *L. infantum* WT cells. Lysates from either untreated (no drug) or phleomycin-treated *L. infantum* WT promastigotes were subjected to western blotting with anti-*Li*BRCA2, anti-hRAD51 or α-tubulin antibodies. Purified (Pur) *Li*BRCA2 or *Li*RAD51 (30 ng) are also shown. pAb, polyclonal antibody; mAb, monoclonal antibody. (**B**) Cytological analysis of *Li*BRCA2–GFP, *Li*RAD51–DsRed, in WT *L. infantum* in the absence of exogenous DNA damage. (**C**) Localization of *Li*RAD51–DsRed in DKO *LiBrca2* in the absence of exogenous DNA damage. The kinetoplast (darker stained disk-shaped structure) and nucleus (lighter stained disk-shaped structure) are stained with DAPI.

tag at the C-terminus of the proteins. Recombinant baculoviruses were used to infect SF9 insect cells, followed by the purification of the recombinant BRCA2 protein. A cell lysate expressing GST–*Li*BRCA2–His was subjected to GST affinity purification followed by GST cleavage with PreScission protease and purification on Talon beads. Opposite to *Li*BRCA2, *Li*RAD51 was well expressed in insect cells and purified by GST affinity purification followed by PreScission cleavage of the GST tag. This led to >95% pure preparations of both *Li*BRCA2 and *Li*RAD51 (Figure 3A).

The native molecular weight of purified *Li*BRCA2 and *Li*RAD51 were determined by gel filtration through Superdex 200 (Figure 3B). Similar to human RAD51 (2), two peaks were observed, in fractions 18–20 (corresponding to an averaged molecular weight of ~350 kDa) and in fractions 28–29 (corresponding to monomeric *Li*RAD51). *Li*BRCA2 eluted in fractions 14–20, with a peak observed

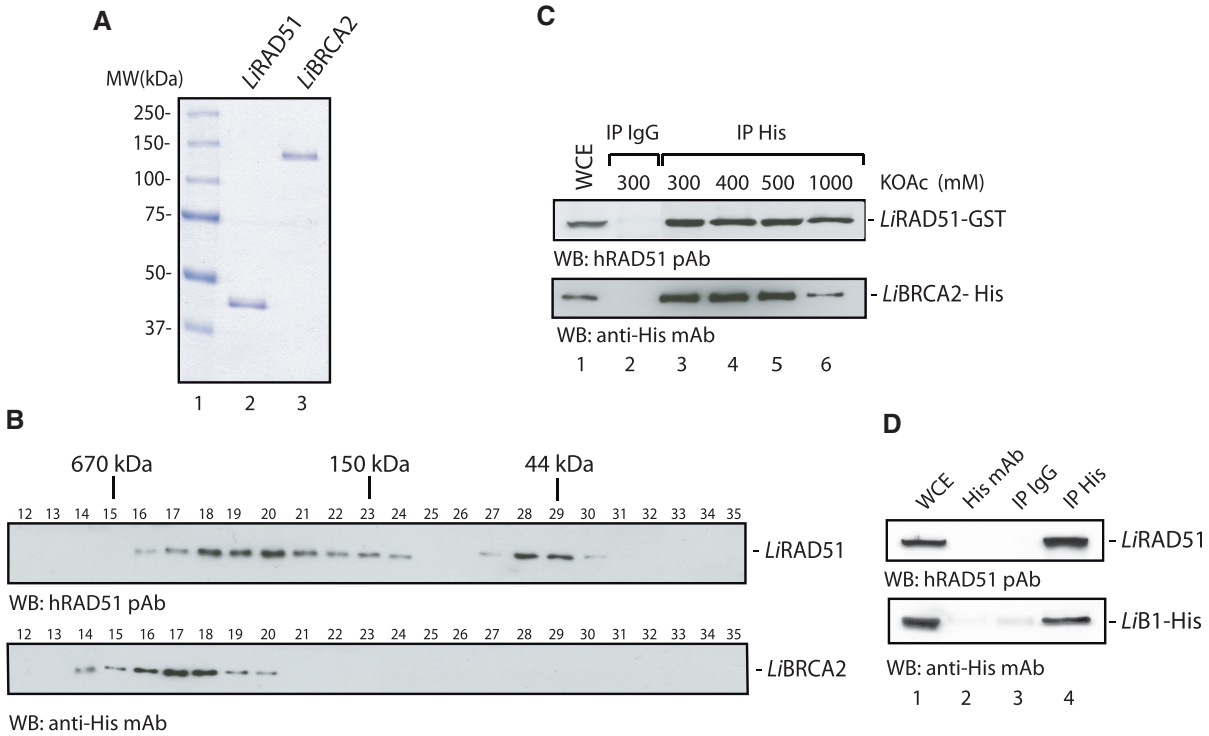

Figure 3. Purification of *L. infantum* RAD51 and BRCA2**.** (**A**) SDS–PAGE of purified *Li*RAD51 and *Li*BRCA2. Purified proteins (400 ng) were loaded on a 8% SDS–PAGE, run then stained with Coomassie blue. Lane 1, molecular weight markers (Bio-Rad); lane 2, purified *Li*RAD51; lane 3, purified *Li*BRCA2. (**B**) Native molecular masses of purified *Li*RAD51 and *Li*BRCA2 as determined by gel filtration through Superdex 200 columns. Eluted fractions 12–35 are presented. Size standards (670, 150 and 44 kDa) are indicated. The upper panel was reacted with an anti-hRAD51 antibody and the bottom panel was revealed with an anti-His antibody. (**C**) *Li*BRCA2 interacts with *Li*RAD51. Sf9 cells were coinfected with *Li*RAD51–GST and *Li*BRCA2–His baculoviruses, followed by immunoprecipitation with IgG alone (lane 2) or anti-His antibody (lanes 3–6). The protein complexes were washed with buffer containing increasing salt (KOAc) concentration, as indicated. Eluted proteins were run onto an SDS–PAGE along with the whole cell extract (lane 1). Blots were reacted with an anti-hRAD51 (upper panel) or anti-His (bottom panel) antibodies. **(D)** The N-terminus of *Li*BRCA2 (*Li*BRCA2–B1) interacts with *Li*RAD51. Immunoprecipitations were conducted as described in (C) from Sf9 cells coinfected with *Li*RAD51–GST and *Li*BRCA2–B1-His baculoviruses. Lane 1, whole cell extract; lane 2, immunoprecipitations with an anti-His antibody alone; lane 3, immunoprecipitations with IgG alone; lane 4, immunoprecipitations with an anti-His antibody. Blots were reacted with anti-hRAD51 polyclonal antibody (upper panel) or with an anti-His monoclonal antibody (bottom panel).

at fractions 17–18 indicative of multimeric forms. This is in agreement with the observation that human BRCA2 forms multimeric rings (21).

As *Li*BRCA2 mediates the recruitment of the recombinase *Li*RAD51 to the nucleus, we therefore tested the possibility that both proteins interact. Using coimmunoprecipitation assays, we observed a co-complex between *Li*RAD51 and *Li*BRCA2 (Figure 3C). The interaction between *Li*BRCA2 and *Li*RAD51 was highly resistant to salt washes (Figure 3C, lanes 3–6). It has been shown that BRC repeats are involved in the interaction between BRCA2 and RAD51. *Leishmania infantum* possesses two BRC repeats located at its N-terminus (Figure 1A and Supplementary Figure S1). To test whether *Li*RAD51 interacts with the N-terminus of *Li*BRCA2, the *Li*BRCA2 N-terminal domain (*Li*BRCA2–B1–His, amino acids 1–122) was coexpressed with *Li*RAD51 in insect cells, followed by immunoprecipitation analysis (Figure 3D). A co-complex between *Li*BRCA2–B1–His and *Li*RAD51 was observed, suggesting that the interaction between *Li*BRCA2 and *Li*RAD51 is mediated through the BRC repeats.

*Li*RAD51 binds DNA, promotes single-strand annealing and strand invasion

As a prerequisite for HR activities, RAD51 binds DNA. *Escherichia coli* RecA protein shows a high affinity for ssDNA compared with duplex DNA, while RAD51 protein binds both ssDNA and dsDNA (40). Using electromobility shift assays, we found that *Li*RAD51 showed similar DNA binding to hRAD51, binding 5'-^{32}P-end-labeled single- and dsDNA with a better affinity for ssDNA (Figure 4A and B, compare lanes 3 and 4). Having established conditions under which *Li*RAD51 bound DNA, we next investigated their ability to promote single-strand annealing. As shown with *Schizosaccharomyces pombe* RAD51 (41), *Li*RAD51 promoted single-strand annealing of complementary ssDNAs of 60 nt. While low levels of spontaneous strand annealing was observed in the control alone (18.2%), *Li*RAD51 formed efficiently renatured DNA products (57.3%) (Figure 4C).

As it is the first time that *Li*RAD51 is analyzed biochemically, it was important to compare its relative activity to human RAD51. First, both proteins were

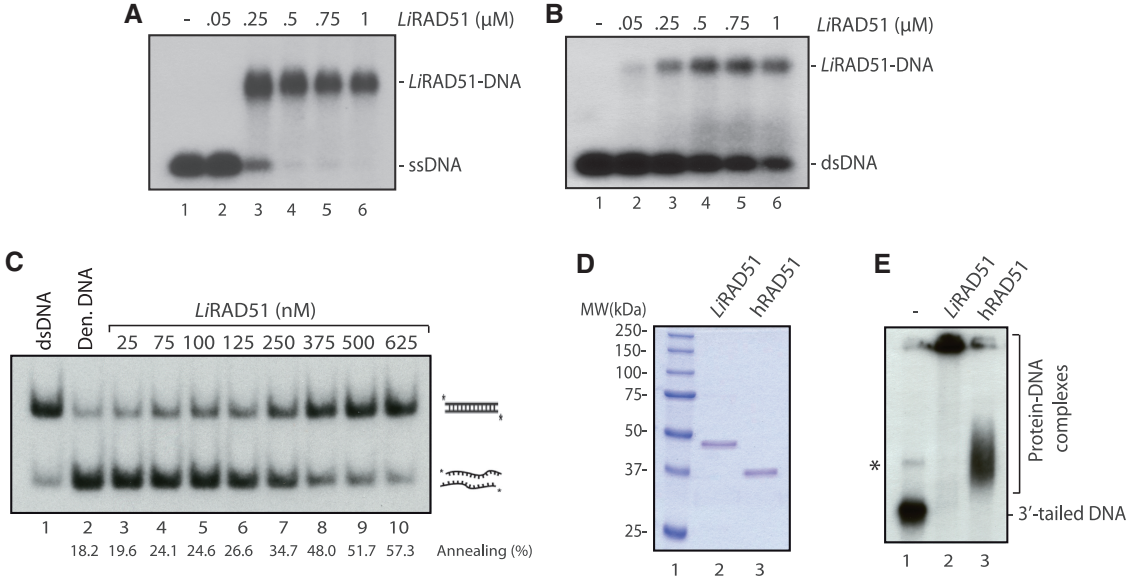

Figure 4. DNA-binding activity of purified *Li*RAD51. (**A**) *Li*RAD51 binds ssDNA. Lanes 1–6, a P^{32}-labeled-60-mer ssDNA was incubated with increasing concentrations of *Li*RAD51 (0–1000 nM). (**B**) *Li*RAD51 binds dsDNA. Lanes 1–6, a P^{32}-labeled-60-mer dsDNA was incubated with increasing concentration of *Li*RAD51 (0–1000 nM). (**C**) *Li*RAD51 is proficient in single-strand annealing. Lane 1, purified 60-bp duplex DNA. Reactions contained denatured 60-bp duplex DNA in buffer with no protein (lane 2) or with purified *Li*RAD51 (25–625 nM), lanes 3–10. The percentage of annealing is indicated at the bottom. (**D**) SDS–PAGE of purified *Li*RAD51 (lane 2) and human RAD51 (lane 3). Molecular weight markers (Bio-Rad) were run in lane 1. Proteins (300 ng) were loaded on a 10% SDS–PAGE and stained with Coomassie blue. (**E**) *Li*RAD51 and human RAD51 show different 3′-tailed DNA-binding profiles. Reactions contained labeled 3′-tailed DNA with no protein (lane 1); with *Li*RAD51 (lane 2); or human RAD51 (lane 3). The asterisk represents annealed 3′-tailed molecules.

quantified to insure that equal amounts of proteins were used in the following experiments (Figure 4D). Since recombination is thought to be initiated by DNA that contains single-stranded tails and these substrates would be subsequently used in D-loop assays, we analyzed the binding of both *Li*RAD51 and hRAD51 to these substrates. While hRAD51 formed complexes of relatively homogeneous size, we observed the formation of *Li*RAD51–DNA networks that tended to smear up the gel (Figure 4E). This result is characteristic of the formation of networks containing a variable number of protein and DNA molecules. A key step in HR is the formation of a D-loop structure, characterized by the invasion of an ssDNA substrate into a homologous duplex DNA (Figure 5A). D-loop assays were performed with long 3′-tailed DNA substrate and homologous supercoiled DNA in magnesium buffer. Adding purified *Li*RAD51 and human RAD51 (200–1200 nM) to these substrates led to an increase of D-loop products in a concentration dependent manner. Quantification of the reaction revealed that *Li*RAD51 was more efficient than human RAD51. At lower concentration (Figure 5B, compare lanes 3–5 and 14–16), *Li*RAD51 was at least 3-fold more efficient than hRAD51. These results show that *Li*RAD51 is a functional recombinase, homologous to hRAD51.

*Li*BRCA2 controls *Li*RAD51 DNA binding

Next, we investigated the DNA-binding properties of *Li*BRCA2. Similar to hBRCA2 (21), *Li*BRCA2 bound ssDNA in a concentration-dependent manner, whereas it did not form stable complexes with dsDNA (Figure 6A and B). Interestingly, *Li*BRCA2 catalyzed the annealing of complementary ssDNAs (Figure 6C). Having established *Li*BRCA2 DNA-binding properties, we next tested whether *Li*BRCA2 affects the DNA-binding affinities of *Li*RAD51. Using conditions where *Li*BRCA2 binding to DNA was minimal (5–20 nM) we observed a significant increase in *Li*RAD51 binding on ssDNA upon the addition of *Li*BRCA2 (Figure 6D). In comparison, *Li*BRCA2 inhibited the loading of *Li*RAD51 on dsDNA (Figure 6E).

In order to better understand how *Li*BRCA2 stimulates *Li*RAD51 DNA-binding ability, we purified a N-terminal fragment of *Li*BRCA2 encompassing amino acids 1–122. This truncation comprises the BRC repeats, but not the OB-fold ssDNA-binding domain. It was recently shown that the BRC5, 6, 7, 8 repeats of human BRCA2 stimulates RAD51 to bind ssDNA (42). At a concentration of 30 nM, 12.1% of ssDNA was bound by *Li*RAD51 (Figure 6F, lane 2). However, when this reaction was supplemented by the *Li*BRCA2 fragment B1 (10–125 nM), *Li*RAD51 bound ssDNA more strongly at all *Li*BRCA2–B1 concentrations (Figure 6F, lanes 4–9), although the stimulation of *Li*RAD51 was more effective at low concentration. Since *Li*BRCA2–B1 does not bind DNA by itself (Figure 6F, lane 3), this result suggests that *Li*BRCA2–B1 stimulates *Li*RAD51–DNA binding through its BRC motifs.

Stimulation of *Li*RAD51 by *Li*BRCA2 and mediator function

By definition, a recombination mediator assists RAD51 to displace the replicative protein A (RPA) to allow RAD51

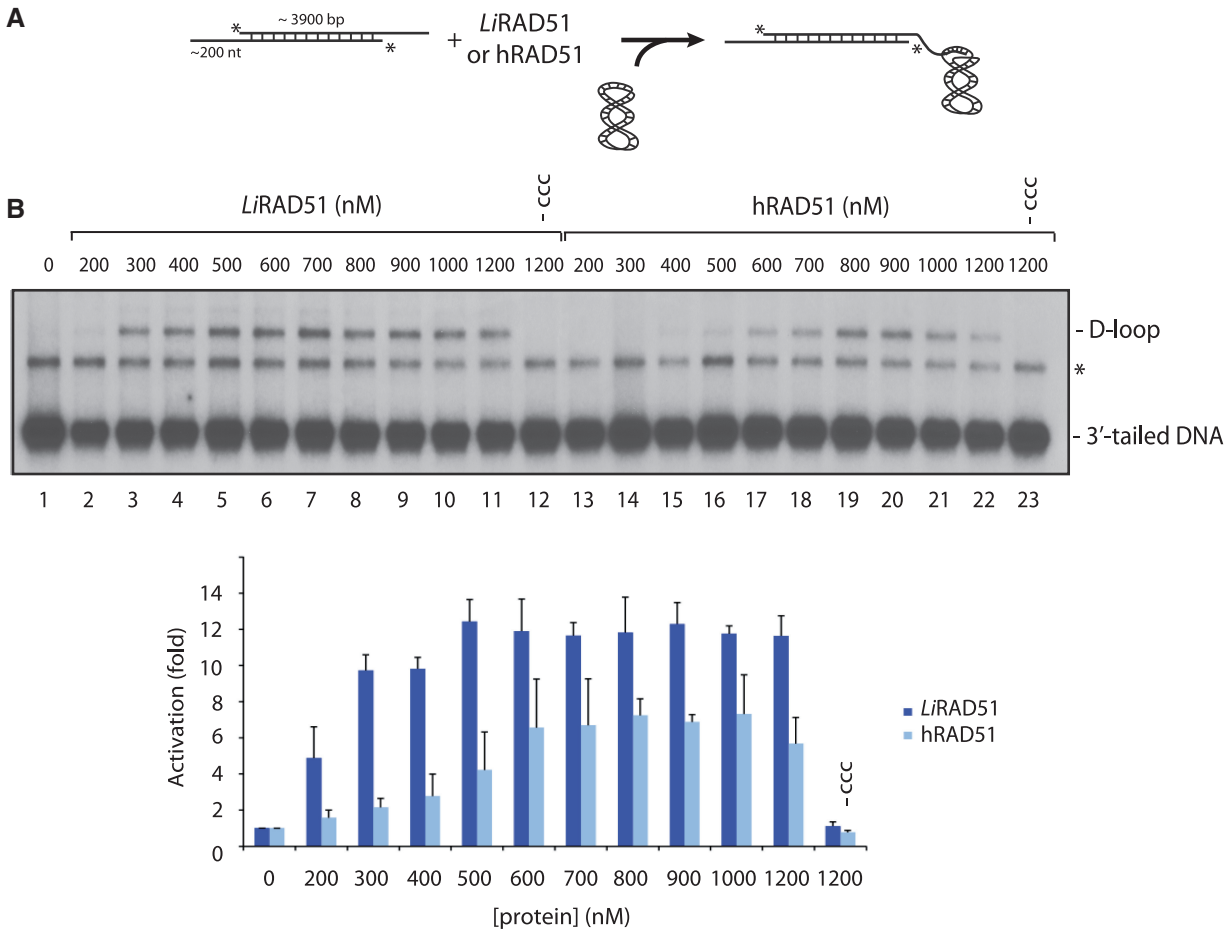

Figure 5. Comparison between *Li*RAD51 and hRAD51 D-loop activities. (**A**) Schematic representation of the D-loop assay using a 4.3-kb resected dsDNA and supercoiled DNA templates. (**B**) Upper panel: D-loop reactions contained the 4.3-kb resected dsDNA with no protein (lane 1), or with purified *Li*RAD51 (200–1200 nM, lanes 2–11). Lane 12 contains *Li*RAD51 (1200 nM) without supercoiled DNA (-ccc). Reactions with human RAD51 (200–1200 nM, lanes 13–22); or human RAD51 (1200 nM) without supercoiled DNA (lane 23) are shown. Lower panel: quantification of results presented in fold activation compared to the control at each protein concentration (nM). The asterisk represents annealed 3′-tailed molecules.

to polymerize as nucleoprotein filaments (43,44). It was previously shown that the *Ustilago maydis* BRCA2 homolog acts as a recombination mediator (45). We therefore tested whether *Li*BRCA2 assisted RAD51 to displace hRPA. In the absence of hRPA, *Li*RAD51 bound beads coated with ssDNA (Figure 7A, lane 4). The addition of hRPA prevented the binding of *Li*RAD51 on ssDNA beads (Figure 7A, lane 5). The addition of *Li*BRCA2 alleviated the inhibitory effect of hRPA, and led to the accumulation of *Li*RAD51 on ssDNA (Figure 7A, lanes 7–8). These results demonstrate that *Li*BRCA2 is a typical recombination mediator. This might be accomplished through interaction with hRPA (Figure 7B).

As *Li*BRCA2 is a recombination mediator, we therefore tested whether it could also stimulate *Li*RAD51 strand invasion ability. When limiting concentrations of *Li*RAD51 were used, only limited D-loop products were produced (Figure 7C, lane 3). However, when *Li*RAD51 was supplemented with *Li*BRCA2 (5–20 nM), strand invasion occurred with a higher level than either protein alone (Figure 7C, compare lanes 4–7 to lanes 2 and 3). No D-loop was observed in the absence of ATP or supercoiled DNA (Figure 7C, lanes 8 and 9). These results show that *Li*BRCA2 promotes *Li*RAD51 activation in D-loop formation, a key step in HR.

DISCUSSION

Mutations in BRCA1 or BRCA2 (BReast CAncer) encoding genes lead to ~10% of familial breast cancers as well as increasing the risk of ovarian cancer. An hallmark of these cancers is genomic instability, characterized by an increase in chromosomal breaks and translocations. In normal cells, this is suppressed by HR which allows the faithful repair of DNA DSBs. The characterization of RAD51 and BRCA2 in a simpler organism such as *L. infantum,* now opens the door to biochemical studies of several aspects of HR, genomic stability and genetic variability.

We showed that *Li*BRCA2 possesses several critical features important for the regulation of DNA recombination. First, using cytological analysis, we observed that

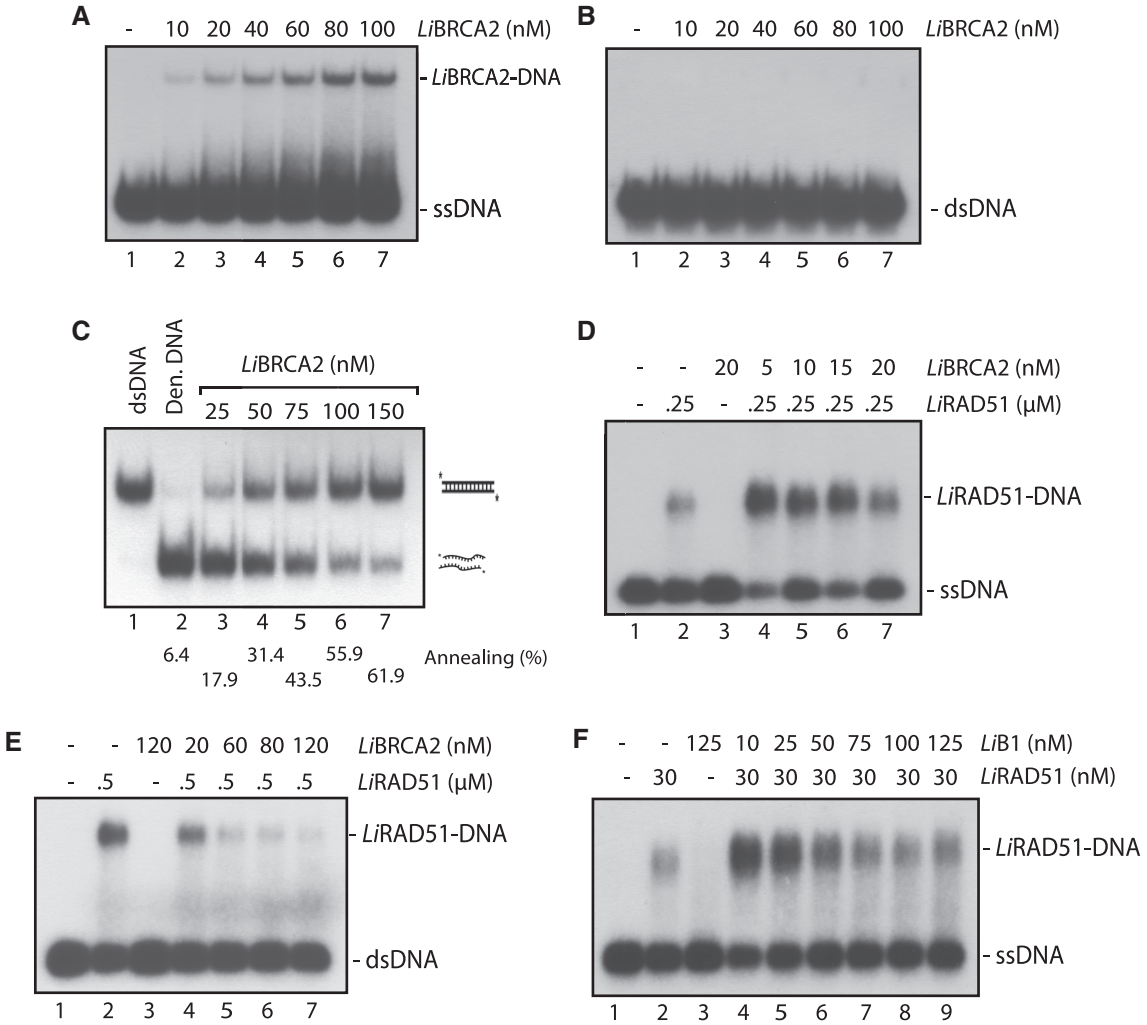

Figure 6. DNA binding, annealing and interacting properties of *Li*BRCA2. (**A**) *Li*BRCA2 binds ssDNA preferentially over dsDNA. A 60-mer ssDNA was incubated with increasing concentration (0–100 nM) of *Li*BRCA2 (lanes 1–7). (**B**) *Li*BRCA2 does not bind 60-mer dsDNA. A 60-mer dsDNA was incubated with increasing concentration (0–100 nM) of *Li*BRCA2 (lanes 1–7) (**C**) *Li*BRCA2 promotes single-strand annealing. Lane 1, purified 60-bp duplex DNA. Reactions (lanes 2–7) contained denatured 60-bp duplex DNA in buffer with an increasing concentration of *Li*BRCA2 (0–150 nM), lanes 2–7. (**D–F**) *Li*BRCA2 stimulates and disrupts *Li*RAD51–dsDNA complexes. (D) *Li*BRCA2 (0–20 nM) was added to pre-assembled *Li*RAD51–ssDNA complexes (with *Li*RAD51 at a concentration of either 0 or 250 nM). (E) *Li*BRCA2 (0–120 nM) was added to pre-assembled *Li*RAD51–dsDNA complexes (with *Li*RAD51 at a concentration of either 0 or 500 nM). (F) The N-terminus of *Li*BRCA2 affects *Li*RAD51 DNA-binding activity. Reactions (lanes 1–9) were conducted as in (D), but using none or 30 nM of *Li*RAD51 and *Li*BRCA2–B1 at concentrations varying between 0 and 125 nM.

*Li*BRCA2 regulates the nuclear accumulation of *Li*RAD51, suggesting a conserved mechanism of nuclear transport by *Li*BRCA2 on *Li*RAD51. The large size of the human BRCA2 protein (384 kDa) poses a great technical challenge for biochemical analyses. To circumvent this problem, we purified a BRCA2 homolog form *L. infantum* which is three times smaller (125 kDa). One key signature of human BRCA2, is eight conserved motifs of approximately 35 amino acids, known as the BRC repeats. We have analyzed the BRCA2 protein sequence of *Leishmania* for the presence of these repeats and generated a BRC repeats tree. Using this analysis we found that *L. infantum*, *T. cruzi*, *L. donovani*, *L. major*, all possessed two BRC repeats, very close to human BRC repeats 7 and 8. This is in contrast with *T. brucei* BRCA2 which contains an expansion of 15 BRC repeats, which is important for RAD51 localization and the efficiency of *T. brucei* HR (46). *Li*BRCA2 also contains one OB-fold domain and a putative Zn-Finger that is unique to the *Leishmania* BRCA2. Recently, the function of the human BRCA2 BRC repeats has been categorized based on their functional mechanisms. BRC1,2,3,4 domains bind to free RAD51 with high avidity, while BRC5, 6, 7, 8 bind poorly free RAD51, but bind the RAD51–ssDNA filament with high affinity (42). Our results show that a fragment of *Li*BRCA2 containing two BRC repeats (related to human BRC repeats 3, 4, 7 and 8, respectively) stimulates *Li*RAD51 binding to ssDNA, especially at low *Li*BRCA2/*Li*RAD51 ratio. At higher *Li*BRCA2/*Li*RAD51 ratios, the enhancement of *Li*RAD51 DNA binding was reduced. This dual mode of regulation has been reported where BRC3 peptide disrupted hRAD51

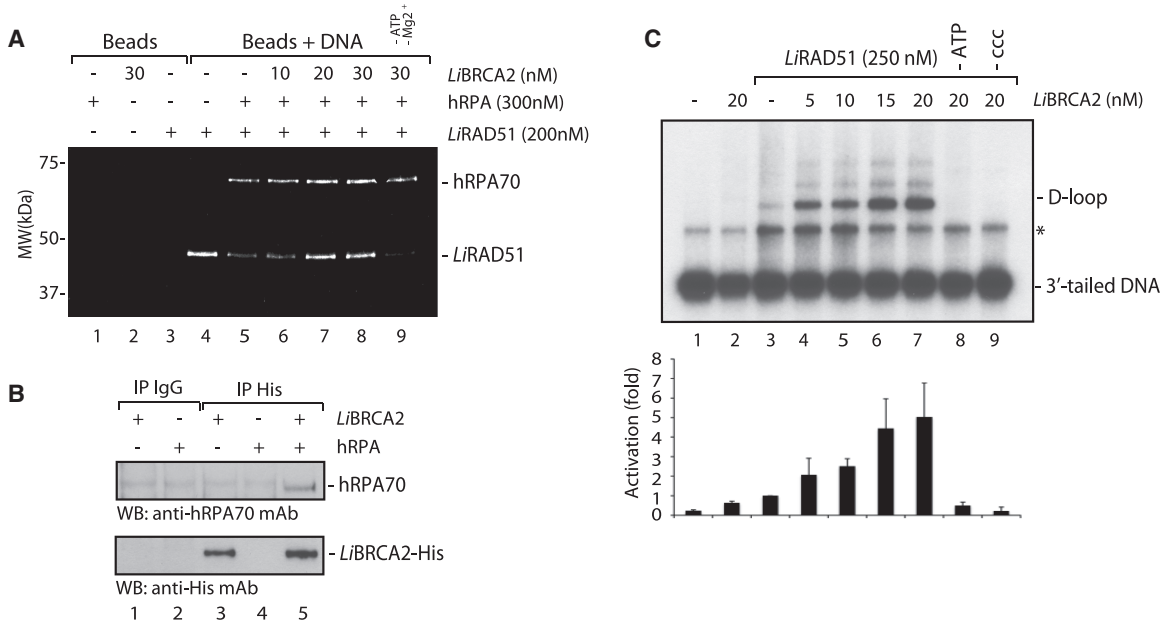

Figure 7. *Li*BRCA2 is a mediator molecule. (**A**) RPA (300 nM) bound to an ssDNA oligonucleotide prevents *Li*RAD51 (200 nM) assembly (lane 5), whereas the addition of *Li*BRCA2 (0–30 nM) stimulates *Li*RAD51 DNA-binding activity in the presence of 300 nM hRPA (lanes 6–8). Background controls demonstrating the interaction of hRPA (lane 1), *Li*BRCA2 (lane 2) and *Li*RAD51 (lane 3) on magnetic beads alone are also shown. The reaction was conducted without ATP and Mg^{2+} in the presence of *Li*BRCA2, hRPA and *Li*RAD51 (lane 9). (**B**) Interaction between *Li*BRCA2 and hRPA. *Li*BRCA2 (750 ng) and/or hRPA (1 μg) were pooled together and coimmunoprecipitation experiments were performed using either IgG (lanes 1 and 2) or His (lanes 3–5) antibodies. Blots were reacted with the indicated antibodies. (**C**) *Li*BRCA2 stimulates *Li*RAD51-catalyzed D-loop formation. Reactions contained DNA alone (lane 1); *Li*BRCA2 (20 nM, lane 2); *Li*RAD51 (250 nM, lanes 3–9); or a combination of both proteins (lanes 4–9) with linear DNA molecule containing 3′-single-strand tails (1 μM). Reactions 8 and 9, do not contain ATP (-ATP) or supercoiled DNA (-ccc), respectively. The asterisk represents annealed 3′-tailed molecules. At the bottom, the intensities of bands obtained for each D-loop reaction were quantified in terms of fold activation compared to the control.

nucleoprotein filaments at high concentration, but formed stable complexes at lower concentration (47). As we observed that *Li*RAD51 levels are very low compared to *Li*BRCA2 without DNA damage, this suggests that *Li*BRCA2 exerts a suppressive role on *Li*RAD51 in normal conditions. However, when *Leishmania* is challenged with DNA damage, *Li*RAD51 levels are increased substantially, suggesting that *Li*BRCA2 might enhance *Li*RAD51-dependent recombination for DNA repair.

During the course of these studies, three independent groups have purified full-length human BRCA2 (21–23). Similar to *Li*BRCA2, it was shown that hBRCA2 is an ssDNA-binding protein (21). However, D-loop formation was not performed for the human BRCA2 protein. In addition, only strand exchange reactions with oligonucleotides, not full-length substrates, were reported. We provide the first evidence of BRCA2 being able to stimulate RAD51-mediated HR by D-loop formation using long DNA substrates. Our results suggest that the minimal domain requirement for a BRCA2 protein to function in such setting is two BRC repeats and an OB-fold.

*Li*BRCA2 is a functional homolog of RAD52

Interestingly, RAD52 is absent in *Leishmania* and *Saccharomyces cerevisiae* does not bear a BRCA2 homolog. In human cells, BRCA2 stimulates the assembly of RAD51 nucleoprotein filament. *Saccharomyces cerevisiae* does not have a BRCA2 homolog and RAD52 is taking charge of this function. Both proteins interact with RPA and RAD51 and their dual inactivation lead to a synthetic lethality phenotype in human cells, demonstrating that both protein mediate pathways leading to RAD51 activation in mammalian cells (48). In *Leishmania*, RAD52 is absent, and BRCA2 might also sustain the function of RAD52 shown in lower organisms. We observed that *Li*BRCA2 stimulated *Li*RAD51 for HR, and interacted with *Li*RAD51 and human RPA. We have not used *Leishmania* RPA or SSB, as the orthologs need to be fully characterized. However, the functional interchangeability between RPA and SSB from different species is supported by results indicating that SSB can substitute for budding yeast and human RPA in strand exchange mediated by *S. cerevisiae* and human RAD51, respectively (49,50). Consistent with the observation that RAD52 deficient cells accumulate genomic instability, we observed that BRCA2 deficient-cells undergo chromosome loss. We also found that *Li*BRCA2 is proficient in single-strand annealing, a function normally attributed to RAD52 (10,51). Thus, our results add significant strength to the idea that BRCA2 is a functional homolog of RAD52 in *Leishmania*.

In order to characterize the function of *Li*BRCA2 *in vivo*, we inactivated BRCA2, and assessed HR and cell survival. Gene targeting was severely affected in the absence of *Li*BRCA2. RNAi approaches are not

functional in *Leishmania* (52), leading to the use of conventional genetic inactivation. DNA integration in *Leishmania* occurs predominantly by HR, whose efficiency can be an obstacle to insertional mutagenesis strategies. Collectively, as well as defining the functions of *Li*BRCA2 and *Li*RAD51, our work also shows that upregulation of HR through overexpression of a recombinase gene might be possible in this unicellular eukaryote.

SUPPLEMENTARY DATA

Supplementary Data are available at NAR Online: Supplementary Table 1, Supplementary Figures 1–3, Supplementary Reference [53].

ACKNOWLEDGEMENTS

The authors would like to thank members of the Masson lab and Danielle Légaré for critical reviewing of the manuscript and members of the Bioimaging Platform of the Centre de Recherche en Infectiologie at the CHUL-CHUQ for their precious help in microscopy-based studies.

FUNDING

CIHR grants (to M.O. and J.Y.M.). M.M.G. is a FQRNT and CIHR Vanier scholar; R.B. is a FQRNT scholar; M.O. holds a Canada Research Chair in Antimicrobial Resistance; J.Y.M. is an FRSQ senior investigator. Funding for open access charge: CIHR.

Conflict of interest statement. None declared.

REFERENCES

1. Moynahan,M.E. and Jasin,M. (2010) Mitotic homologous recombination maintains genomic stability and suppresses tumorigenesis. *Nat. Rev. Mol. Cell. Biol.*, **11**, 196–207.
2. Davies,A.A., Masson,J.Y., McIlwraith,M.J., Stasiak,A.Z., Stasiak,A., Venkitaraman,A.R. and West,S.C. (2001) Role of BRCA2 in control of the RAD51 recombination and DNA repair protein. *Mol. Cell.*, **7**, 273–282.
3. Esashi,F., Christ,N., Gannon,J., Liu,Y., Hunt,T., Jasin,M. and West,S.C. (2005) CDK-dependent phosphorylation of BRCA2 as a regulatory mechanism for recombinational repair. *Nature*, **434**, 598–604.
4. Esashi,F., Galkin,V.E., Yu,X., Egelman,E.H. and West,S.C. (2007) Stabilization of RAD51 nucleoprotein filaments by the C-terminal region of BRCA2. *Nat. Struct. Mol. Biol.*, **14**, 468–474.
5. Carreira,A., Hilario,J., Amitani,I., Baskin,R.J., Shivji,M.K., Venkitaraman,A.R. and Kowalczykowski,S.C. (2009) The BRC repeats of BRCA2 modulate the DNA-binding selectivity of RAD51. *Cell*, **136**, 1032–1043.
6. Yang,H., Jeffrey,P.D., Miller,J., Kinnucan,E., Sun,Y., Thoma,N.H., Zheng,N., Chen,P.L., Lee,W.H. and Pavletich,N.P. (2002) BRCA2 function in DNA binding and recombination from a BRCA2-DSS1-ssDNA structure. *Science*, **297**, 1837–1848.
7. Bochkarev,A. and Bochkareva,E. (2004) From RPA to BRCA2: lessons from single-stranded DNA binding by the OB-fold. *Curr. Opin. Struct. Biol.*, **14**, 36–42.
8. Lo,T., Pellegrini,L., Venkitaraman,A.R. and Blundell,T.L. (2003) Sequence fingerprints in BRCA2 and RAD51: implications for DNA repair and cancer. *DNA Repair*, **2**, 1015–1028.
9. Passos-Silva,D.G., Rajão,M.A., Nascimento de Aguiar,P.H., Vieira-da-Rocha,J.P., Machado,C.R. and Furtado,C. (2010) Overview of DNA repair in Trypanosoma cruzi, Trypanosoma brucei, and Leishmania major. *J. Nucleic Acids*, **2010**, 840768.
10. Mortensen,U.H., Bendixen,C., Sunjevaric,I. and Rothstein,R. (1996) DNA strand annealing is promoted by the yeast Rad52 protein. *Proc. Natl Acad. Sci. USA*, **93**, 10729–10734.
11. Shinohara,A., Shinohara,M., Ohta,T., Matsuda,S. and Ogawa,T. (1998) Rad52 forms ring structures and co-operates with RPA in single-strand DNA annealing. *Genes Cells*, **3**, 145–156.
12. Shen,Z., Cloud,K.G., Chen,D.J. and Park,M.S. (1996) Specific interactions between the human Rad51 and Rad52 proteins. *J. Biol. Chem.*, **271**, 148–152.
13. Conway,C., Proudfoot,C., Burton,P., Barry,J.D. and McCulloch,R. (2002) Two pathways of homologous recombination in Trypanosoma brucei. *Mol. Microbiol.*, **45**, 1687–1700.
14. Janzen,C.J., Lander,F., Dreesen,O. and Cross,G.A. (2004) Telomere length regulation and transcriptional silencing in KU80-deficient Trypanosoma brucei. *Nucleic Acids Res.*, **32**, 6575–6584.
15. Burton,P., McBride,D.J., Wilkes,J.M., Barry,J.D. and McCulloch,R. (2007) Ku heterodimer-independent end joining in Trypanosoma brucei cell extracts relies upon sequence microhomology. *Eukaryotic Cell*, **6**, 1773–1781.
16. Boothroyd,C.E., Dreesen,O., Leonova,T., Ly,K.I., Figueiredo,L.M., Cross,G.A. and Papavasiliou,F.N. (2009) A yeast-endonuclease-generated DNA break induces antigenic switching in Trypanosoma brucei. *Nature*, **459**, 278–281.
17. Ubeda,J.M., Légaré,D., Raymond,F., Ouameur,A.A., Boisvert,S., Rigault,P., Corbeil,J., Tremblay,M.J., Olivier,M., Papadopoulou,B. *et al.* (2008) Modulation of gene expression in drug resistant Leishmania is associated with gene amplification, gene deletion and chromosome aneuploidy. *Genome Biol.*, **9**, R115.
18. Mazloum,N., Zhou,Q. and Holloman,W.K. (2007) DNA binding, annealing, and strand exchange activities of Brh2 protein from Ustilago maydis. *Biochemistry*, **46**, 7163–7173.
19. Mazloum,N., Zhou,Q. and Holloman,W.K. (2008) D-loop formation by Brh2 protein of Ustilago maydis. *Proc. Natl Acad. Sci. USA*, **105**, 524–529.
20. Mazloum,N. and Holloman,W.K. (2009) Second-end capture in DNA double-strand break repair promoted by Brh2 protein of Ustilago maydis. *Mol. Cell.*, **33**, 160–170.
21. Thorslund,T., McIlwraith,M.J., Compton,S.A., Lekomtsev,S., Petronczki,M., Griffith,J.D. and West,S.C. (2010) The breast cancer tumor suppressor BRCA2 promotes the specific targeting of RAD51 to single-stranded DNA. *Nat. Struct. Mol. Biol.*, **17**, 1263–1265.
22. Liu,J., Doty,T., Gibson,B. and Heyer,W.D. (2010) Human BRCA2 protein promotes RAD51 filament formation on RPA-covered single-stranded DNA. *Nat. Struct. Mol. Biol.*, **17**, 1260–1262.
23. Jensen,R.B., Carreira,A. and Kowalczykowski,S.C. (2010) Purified human BRCA2 stimulates RAD51-mediated recombination. *Nature*, **467**, 678–683.
24. McKean,P.G., Keen,J.K., Smith,D.F. and Benson,F.E. (2001) Identification and characterisation of a RAD51 gene from Leishmania major. *Mol. Biochem. Parasitol.*, **115**, 209–216.
25. Papadopoulou,B., Roy,G. and Ouellette,M. (1992) A novel antifolate resistance gene on the amplified H circle of Leishmania. *EMBO J.*, **11**, 3601–3608.
26. Mukherjee,A., Roy,G., Guimond,C. and Ouellette,M. (2009) The gamma-glutamylcysteine synthetase gene of Leishmania is essential and involved in response to oxidants. *Mol. Microbiol.*, **74**, 914–927.
27. El Fadili,A., Kündig,C. and Ouellette,M. (2002) Characterization of the folylpolyglutamate synthetase gene and polyglutamylation of folates in the protozoan parasite Leishmania. *Mol. Biochem. Parasitol.*, **124**, 63–71.
28. Richard,D., Leprohon,P., Drummelsmith,J. and Ouellette,M. (2004) Growth phase regulation of the main folate transporter of

Leishmania infantum and its role in methotrexate resistance. *J. Biol. Chem.*, **279**, 54494–54501.
29. Sambrook,E.F., Fritsch,E.F. and Maniatis,T. (1989) *Molecular Cloning: A Laboratory Manual*. Cold Spring Harbor Laboratory Press, Cold Spring Harbor, New York.
30. Eddy,S.R. (1998) Profile hidden Markov models. *Bioinformatics*, **14**, 755–763.
31. Waterhouse,A.M., Procter,J.B., Martin,D.M., Clamp,M. and Barton,G.J. (2009) Jalview Version 2–a multiple sequence alignment editor and analysis workbench. *Bioinformatics*, **25**, 1189–1191.
32. Katoh,K., Misawa,K., Kuma,K. and Miyata,T. (2002) MAFFT: a novel method for rapid multiple sequence alignment based on fast Fourier transform. *Nucleic Acids Res.*, **30**, 3059–3066.
33. Katoh,K., Kuma,K., Toh,H. and Miyata,T. (2005) MAFFT version 5: improvement in accuracy of multiple sequence alignment. *Nucleic Acids Res.*, **33**, 511–518.
34. Henricksen,L.A., Umbricht,C.B. and Wold,M.S. (1994) Recombinant replication protein A: expression, complex formation, and functional characterization. *J. Biol. Chem.*, **269**, 11121–11132.
35. Baumann,P., Benson,F.E., Hajibagheri,N. and West,S.C. (1997) Purification of human Rad51 protein by selective spermidine precipitation. *Mutat. Res.*, **384**, 65–72.
36. Buisson,R., Dion-Côté,A.M., Coulombe,Y., Launay,H., Cai,H., Stasiak,A.Z., Stasiak,A., Xia,B. and Masson,J.Y. (2010) Cooperation of breast cancer proteins PALB2 and piccolo BRCA2 in stimulating homologous recombination. *Nat. Struct. Mol. Biol.*, **17**, 1247–1254.
37. Masson,J.Y., Davies,A.A., Hajibagheri,N., Van Dyck,E., Benson,F.E., Stasiak,A.Z., Stasiak,A. and West,S.C. (1999) The meiosis-specific recombinase hDmc1 forms rings structures and interacts with hRad51. *EMBO J.*, **18**, 6552–6560.
38. Suzuki,A., de la Pompa,J.L., Hakem,R., Elia,A., Yoshida,R., Mo,R., Nishina,H., Chuang,T., Wakeham,A., Itie,A. *et al.* (1997) Brca2 is required for embryonic cellular proliferation in the mouse. *Genes Dev.*, **11**, 1242–1252.
39. Yu,V.P., Koehler,M., Steinlein,C., Schmid,M., Hanakahi,L.A., van Gool,A.J., West,S.C. and Venkitaraman,A.R. (2000) Gross chromosomal rearrangements and genetic exchange between nonhomologous chromosomes following BRCA2 inactivation. *Genes Dev.*, **14**, 1400–1406.
40. Benson,F.E., Stasiak,A. and West,S.C. (1994) Purification and characterization of the human Rad51 protein, an analogue of E. coli RecA. *EMBO J.*, **13**, 5764–5771.
41. Sauvageau,S., Stasiak,A.Z., Banville,I., Ploquin,M., Stasiak,A. and Masson,J.Y. (2005) Fission yeast rad51 and dmc1, two efficient DNA recombinases forming helical nucleoprotein filaments. *Mol. Cell. Biol*, **25**, 4377–4387.
42. Carreira,A. and Kowalczykowski,S.C. (2011) Two classes of BRC repeats in BRCA2 promote RAD51 nucleoprotein filament function by distinct mechanisms. *Proc. Natl Acad. Sci. USA*, **108**, 10448–10453.
43. Sung,P. (2005) Mediating repair. *Nat. Struct. Mol. Biol.*, **12**, 213–214.
44. Schild,D. and Wiese,C. (2010) Overexpression of RAD51 suppresses recombination defects: a possible mechanism to reverse genomic instability. *Nucleic Acids Res.*, **38**, 1061–1070.
45. Yang,H., Li,Q., Fan,J., Holloman,W.K. and Pavletich,N.P. (2005) The BRCA2 homologue Brh2 nucleates RAD51 filament formation at a dsDNA-ssDNA junction. *Nature*, **433**, 653–657.
46. Hartley,C.L. and McCulloch,R. (2008) Trypanosoma brucei BRCA2 acts in antigenic variation and has undergone a recent expansion in BRC repeat number that is important during homologous recombination. *Mol. Microbiol.*, **68**, 1237–1251.
47. Galkin,V.E., Esashi,F., Yu,X., Yang,S., West,S.C. and Egelman,E.H. (2005) BRCA2 BRC motifs bind RAD51-DNA filaments. *Proc. Natl Acad. Sci. USA*, **102**, 8537–8542.
48. Feng,Z., Scott,S.P., Bussen,W., Sharma,G.G., Guo,G., Pandita,T.K. and Powell,S.N. (2011) Rad52 inactivation is synthetically lethal with BRCA2 deficiency. *Proc. Natl Acad. Sci. USA*, **108**, 686–691.
49. Sugiyama,T., Zaitseva,E.M. and Kowalczykowski,S.C. (1997) A single-stranded DNA-binding protein is needed for efficient presynaptic complex formation by the Saccharomyces cerevisiae Rad51 protein. *J. Biol. Chem.*, **272**, 7940–7945.
50. Baumann,P. and West,S.C. (1999) Heteroduplex formation by human Rad51 protein: effects of DNA end-structure, hRP-A and hRad52. *J. Mol. Biol.*, **291**, 363–374.
51. Ploquin,M., Bransi,A., Paquet,E.R., Stasiak,A.Z., Stasiak,A., Yu,X., Cieslinska,A.M., Egelman,E.H., Moineau,S. and Masson,J.Y. (2008) Functional and structural basis for a bacteriophage homolog of human RAD52. *Curr. Biol*, **18**, 1142–1146.
52. Robinson,K.A. and Beverley,S.M. (2003) Improvements in transfection efficiency and tests of RNA interference (RNAi) approaches in the protozoan parasite Leishmania. *Mol. Biochem. Parasitol.*, **128**, 217–228.
53. Crooks,G.E., Hon,G., Chandonia,J.M. and Brenner,S.E. (2004) WebLogo: a sequence logo generator. *Genome Res*, **14**, 1188–1190.